



Longitudinal multimodal imaging of bilateral diffuse uveal melanocytic proliferation secondary to gallbladder adenocarcinoma

Shaman Dolly^{a,b}, Christiana Dinah^{b,*}

^a Royal London Hospital, Barts Health NHS Trust, Whitechapel, Whitechapel Road, London, E1 1FR, United Kingdom

^b Central Middlesex Hospital, London North West Healthcare NHS Trust, Acton Lane, London, NW10 7NS, United Kingdom

ARTICLE INFO

Keywords:

Uveal melanocytic proliferation
Paraneoplastic
Leopard spot retinopathy
Multimodal imaging
Bacillary detachment

ABSTRACT

Purpose: To present the longitudinal, multimodal imaging of Bilateral Diffuse Uveal Melanocytic Proliferation secondary to gallbladder carcinoma over a 17 month period, demonstrating the natural history, the evolution with treatment and salient features to support timely diagnosis of this condition with life-threatening associations.

Observations: A systemically well 73 year old woman presented with a 2 month history of progressive visual loss in the right eye. We report the initial findings on clinical examination and with retinal imaging including fluorescein and indocyanine angiography, optical coherence tomography and autofluorescence. An initial diagnosis of atypical central serous chorioretinopathy with secondary choroidal neovascularisation led to treatment with intravitreal aflibercept before the correct diagnosis of BDUMP was made 2 months later, aided by evolution of signs on imaging and examination. Subsequent investigation led to detection of gallbladder adenocarcinoma. The patient underwent systemic chemotherapy and eventual phacoemulsification and insertion of intraocular lens to both eyes. The patient died 21 months after presentation of visual symptoms, with latest imaging at 17 months.

Conclusion: We report the evolution of BDUMP utilising multi-modal imaging pre-treatment and during treatment with chemotherapy, and highlight peripheral progression of disease despite consolidation at the macula.

1. Introduction

Bilateral Diffuse Uveal Melanocytic Proliferation (BDUMP) is a paraneoplastic syndrome, the five cardinal clinical signs of which are 1) multifocal faint, round or oval red, subretinal patches; 2) associated hyperfluorescence during early angiography; 3) development of multiple, slightly elevated, pigmented and non-pigmented uveal melanocytic tumors as evidenced by diffuse thickening of the uveal tract; 4) exudative retinal detachment; and 5) rapid progression of cataract.¹

It remains rare, with only around one hundred cases in the literature to date. We describe a case associated with gallbladder adenocarcinoma, an uncommonly associated primary malignancy,² and present, across 17 months of follow-up, comprehensive multimodal imaging of its clinical course. Our case highlights the difficulties in making an early diagnosis of BDUMP. More familiarity with the imaging features may lead to

sooner diagnosis and management. This is important for both ophthalmic and oncology staff, as the disease can present before and after the primary tumor has been found.

2. Case report

A 73 year old Caucasian woman presented to the retina clinic with a 2 month history of gradual right eye visual blurring. She denied other ocular or systemic symptoms, and had a medical history positive for hypertension and rheumatoid arthritis. Best corrected visual acuity (BCVA) was Snellen 20/50 in the right eye and 20/25 in the left eye, with normal intraocular pressures.

On examination, pale, confluent subretinal yellowish discoloration of both maculae were noted along with multiple faint, flat pigmented lesions presumed to be choroidal nevi.

* Corresponding author. Central Middlesex Hospital, London North West Healthcare NHS Trust, Acton Lane, London, NW10 7NS, United Kingdom.

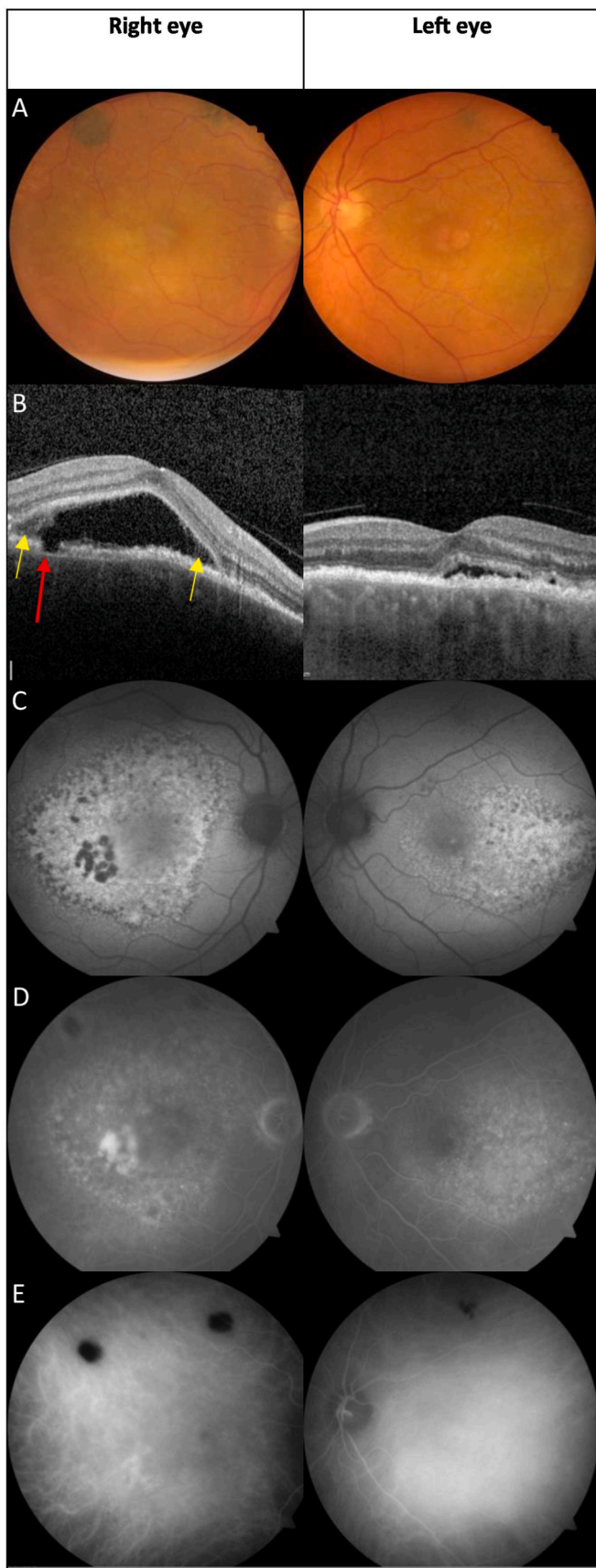
E-mail addresses: shaman.dolly1@nhs.net (S. Dolly), christiana.dinah@nhs.net (C. Dinah).

<https://doi.org/10.1016/j.ajoc.2024.102103>

Received 17 January 2024; Received in revised form 6 June 2024; Accepted 29 June 2024

Available online 21 July 2024

2451-9936/© 2024 The Authors. Published by Elsevier Inc. This is an open access article under the CC BY-NC-ND license (<http://creativecommons.org/licenses/by-nc-nd/4.0/>).



(caption on next column)

Fig. 1. Multimodal imaging of right and left eyes at presentation, 2 months after initial symptom onset.

A) Macula centred colour fundus photograph with yellow confluent subretinal lesions at the maculae and choroidal pigmented lesions visible superiorly.

B) Macula OCT b scan images. Right eye - Large area of subretinal fluid with thickening of RPE, interspersed with thinning and a focal area of complete loss of RPE (red arrow) with moderately hyperreflective material in the adjacent subretinal space (yellow arrow). Left eye - Similar thickening and thinning of RPE with shallow subretinal fluid.

C) fundus autofluorescence demonstrating the leopard spot appearance of alternating areas of hyper-autofluorescence and hypo-autofluorescence. There is hypo autofluorescence of the confluent nummular lesions temporal to the fovea.

D) Late phase FFA images demonstrating multifocal areas patchy hyperfluorescence and staining of the nummular lesions temporal to the fovea. Focal areas of hypo fluorescence superiorly correspond to choroidal nevi

E) Late phase ICG images demonstrating hypo fluorescence corresponding to the pigmented choroidal lesions. Dilated, hyperpermeable choroidal vessels are also evident. (For interpretation of the references to colour in this figure legend, the reader is referred to the Web version of this article.)

Spectral domain optical coherence tomography (SD-OCT) scan (Spectralis, Heidelberg Engineering, Heidelberg, Germany) demonstrated bilateral serous retinal detachment at the macula, greater in the right eye, with retinal pigment epithelium (RPE) thickening, interspersed with thinning and bilateral choroidal thickening. Fundus Autofluorescence (Visucam 200, Zeiss, Oberkochen, Germany) demonstrated bilateral alternating areas of hyper-autofluorescence and hypo-autofluorescence.

Fundus fluorescein angiography (Visucam 200, Zeiss, Oberkochen, Germany) demonstrated multifocal areas of patchy hyperfluorescence and hypofluorescence with focal staining corresponding to the area of amorphous hyperreflective material on OCT. Indocyanine green demonstrated dilated, hyperpermeable vessels and hypofluorescence corresponding to the presumed choroidal nevi (Fig. 1).

A provisional diagnosis of atypical bilateral chronic central serous chorioretinopathy (CSCR) was made, with possible secondary choroidal neovascularisation (CNV) in the right eye.

The patient was initiated on a course of three aflibercept (Eylea, Regeneron) intravitreal injections at 4 weekly intervals in the right eye.

On examination on the day of the third injection, the choroidal pigmented lesions had increased in number and size and SD-OCT review confirmed persistent subretinal fluid associated with bacillary layer serous retinal detachment (Fig. 2). Of note, the near infrared image demonstrated a leopard-spot pattern of hyper and hypo reflectivity (Fig. 3). These findings appeared consistent with a diagnosis of bilateral diffuse uveal melanocytic proliferation (BDUMP) and the patient was referred to a tertiary ocular oncology centre.

Initial whole body computed tomography imaging did not reveal an underlying tumor, but positron emission tomography demonstrated high uptake near the gallbladder, and lymph node fine needle aspirate (FNA) biopsy confirmed gallbladder adenocarcinoma, regionally metastatic to the lymph nodes. Immunohistochemistry demonstrated poorly differentiated adenocarcinoma cytokeratin (CK) 7 +ve, CK20 -ve.

MRI head and orbit showed bilateral uveal thickening and contrast enhancement suggesting melanocytic proliferation with no extraocular or orbital involvement.

Blood tests on referral to oncologists showed no abnormality, but later a raised alkaline phosphatase of 166 IU/L was found.

Surgical management was contraindicated due to proximity of tumor to the hepatic vessels and aorta. The patient was initiated on chemotherapy 9 months following her initial presentation to eye services.

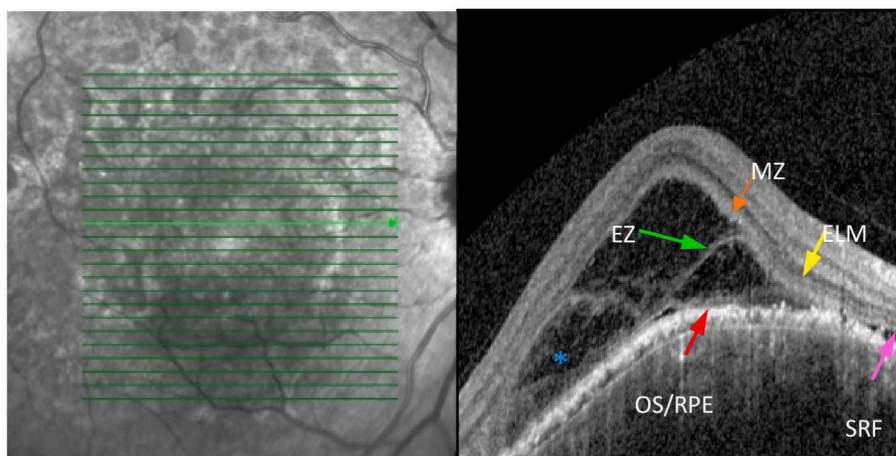


Fig. 2. Near infrared and OCT - scan image of the right macula after 3 intravitreal aflibercept injections at 4 weekly intervals.

A) Leopard spot pattern of macula on near infra-red image.

B) Bacillary layer retinal detachment. The hyperreflective external limiting membrane (ELM) (yellow arrow) can be seen and posterior to this, the hyporeflective myoid zone (MZ) where a split occurs from the underlying ellipsoid zone (EZ) creating a fluid-filled cavity. Beneath this is a faintly hyper reflective line above the RPE which is the outer segment/RPE (OS/RPE) complex. Subretinal fluid (SRF) can be seen nasally (pink arrow).

Moderately hyperreflective material likely demonstrating photoreceptor segments sheared at various levels is seen in the fluid-filled cavity (*). (For interpretation of the references to colour in this figure legend, the reader is referred to the Web version of this article.)

3. Clinical progression

4 months after starting chemotherapy, SD-OCT demonstrated significant but incomplete resolution of subretinal fluid in the right macula, with thickening of the RPE throughout the posterior pole. At the left macula, there was evidence of similar thickening and irregularity of the RPE away from the fovea, with residual subretinal fluid and further foveal RPE and photoreceptor atrophy (Fig. 4).

As illustrated in Fig. 3, the leopard spot appearance of alternating hyperpigmented and hypopigmented areas of the RPE continued to expand outside of the macula to the inferior retina, followed by simultaneous involvement of the nasal and temporal peripheral retina.

Cataracts developed and rapidly progressed during her treatment course, and the patient underwent phacoemulsification and insertion of intraocular lens (Phaco IOL) procedures to both eyes sequentially.

Despite treatment, the patient died 21 months after presentation, 12 months after starting chemotherapy, with a final recorded visual acuity before her right phaco IOL of 20/2400 right and 20/50 left (Fig. 5).

4. Discussion

The appearance of reticulated depigmentation as in our patient lends its name to ‘leopard’ or ‘giraffe’ spot retina which has numerous differentials, though the presence of multifocal pigmented choroidal tumors is an important differentiator. Malignant manifestations include cancer associated retinopathy, metastatic uveal deposits, leukemic infiltration and lymphoma.³ Benign differentials include choroidal melanocytosis, chronic CSCR, acute polymorphous vitelliform maculopathy, choroiditis, hypertrophy of the RPE, resolved chronic retinal detachment or uveal effusion syndrome, amongst others.⁴ Importantly, we illustrate the evolution of BDUMP before and after chemotherapy, with multimodal imaging. Autofluorescence imaging is the most striking demonstration of the retinal changes and may best aid diagnosis at an

earlier stage. The leopard-spot pattern is also noted on near-infrared imaging early in the disease (Fig. 2).

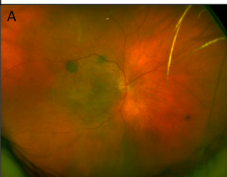
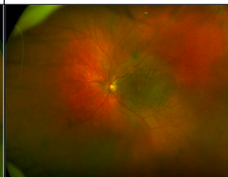
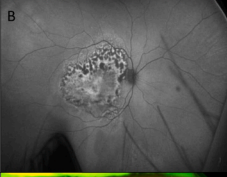
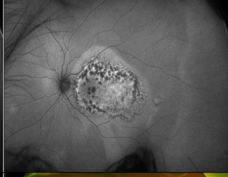
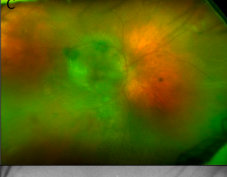
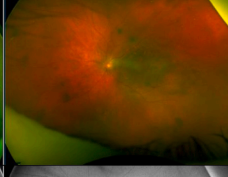
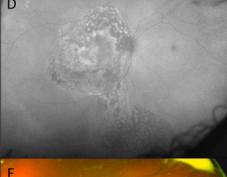
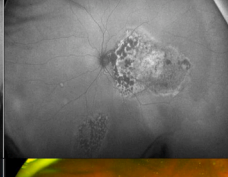
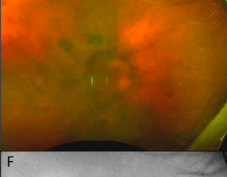
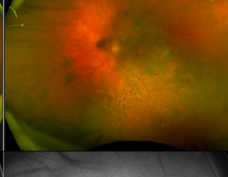
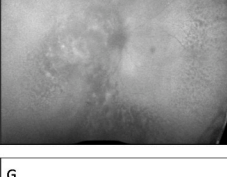
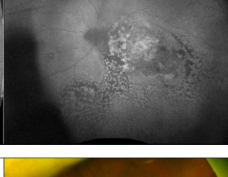

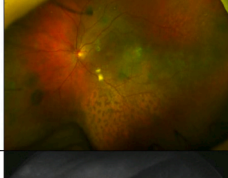

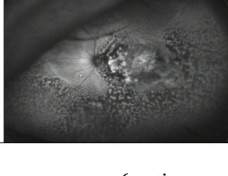
On SD-OCT, we highlight the presence of bacillary layer retinal detachments, first formally described in BDUMP by Breazzano et al.⁵ This is a previously noticed phenomena in OCT scans of BDUMP, though not all authors comment explicitly on the appearance despite its presence.^{6,7} Bacillary layer detachments have been seen in other macula diseases including Vogt-Koyanagi-Harada disease, neovascular age-related macula degeneration and pachychoroid disease.⁸

Hallmarks are co-localisation of subretinal fluid and enhanced features of the outer retina. The fluid accumulates above the RPE and within the photoreceptor layer, likely at the myoid portion of the inner segments (IS) which split from the outer segments (OS) which are still attached to the RPE-basal lamina-Bruchs membrane complex.⁸ Fluid and fibrin accumulation occurs under the external limiting membrane (ELM) and myoid zone, separating the photoreceptor segments.⁵ It is believed that choroidal ischemia and resultant RPE dysfunction, exudation and vascular permeability are contributory mechanisms to the fluid. Our patient shows a split at the level of both the ELM and the IS/OS junction (Fig. 2).

As the subretinal fluid resolves in our case, there is increased subretinal hyper-reflectivity resembling a subretinal fibrosis-like process in addition to ongoing RPE thickening.

Despite reduction in macular subretinal fluid in both eyes on chemotherapy, peripheral retinal changes progressed as shown in the ultra-wide fundus photography and autofluorescence. The pattern of progressive inferior RPE lesions following macula lesions may suggest a migration of fluid in a similar way to the gravitational tracts seen in CSCR, with associated underlying RPE involvement at areas of serous detachment.

The aetiology of BDUMP is uncertain but is thought to be caused by either a tumor secreted or immune mediated molecule.⁹⁻¹¹ Considering this, our hypothesis is that the pigmented RPE lesions occur

Time point	Right eye	Left eye	Visual Acuity
4 months after presentation			Right 20/60 Left 20/40
			
10 months after presentation, 1 month after chemotherapy			Right 20/125 Left 20/40
			
14 months after presentation, 5 month after chemotherapy			Right 20/1200 Left 20/60
			
17 months after presentation, 8 month after chemotherapy			Right 20/2400 Left 20/40
			

(caption on next column)

Fig. 3. Ultrawidefield pseudocolour fundus photo and autofluorescence images at numerous timepoints.

A) RPE pigmented lesions seen at the macula and peripherally resulting in a leopard spot appearance of the macula.

B) Alternating areas of hyper and hypo-autofluorescence localised to the macula of both eyes.

C) Enlargement and increase in leopard spot retinal appearance extending beyond the macula, including inferiorly in the right eye.

D) Alternating pattern of autofluorescence has extended across the posterior pole with:

Right - Areas of hypo-autofluorescence enlarging and becoming confluent. A second localised collection is seen in the inferior peripheral retina connected by a gravitational tract. Note the image is obscured by lenticular opacity.

Left - a new localised discrete inferonasal area of similar alternating autofluorescence.

E) Further enlargement and increase in leopard spot appearance notable temporally and nasally on the right, and inferiorly on the left. Right eye is significantly obscured by a posterior sub-capsular cataract.

F) Right - alternating pattern of autofluorescence has further expanded at the posterior pole and temporally past the macula. The inferior areas of hypo-autofluorescence have become greater and more confluent and a large area of peripheral nasal retina has developed the pattern of autofluorescence, possibly connected to the existing inferior area.

Left - Area of alternating autofluorescence has enlarged and coalesced with the previous discrete area and involved a significant area of the temporal retina.

G) Left fundus after phacoemulsification and insertion of intraocular lens. The pigmented RPE lesions are visible throughout the majority of the temporal and inferior retina.

H) Left - alternating pattern of autofluorescence involves the majority of the inferior and temporal retina.

Note - No image is available for the right eye at month 17 after presentation as a fundus-obscuring cataract is present.

simultaneously in multiple areas of the retina, but present initially in the macula due to it having the highest blood flow and therefore tissue exposure to the causative molecule.

Management of BDUMP is primarily of the underlying tumor, with some patients demonstrating improvement with plasmapheresis and others not.^{6,11-13} The difference in efficacy may lie in that a small molecule growth factor may be causative, as opposed to an immune mediated molecule. Where large molecular weight, intravascular, and slowly produced molecules such as immunoglobulins favor response to plasmapheresis removal, small molecules rapidly produced by the tumor

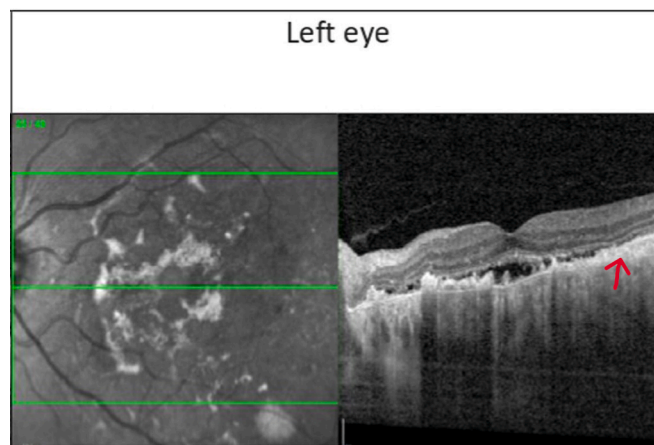


Fig. 4. Near infrared photographs and fovea bisecting OCT b-scan images of the left macula at month 13 after presentation, month 4 after chemotherapy, before cataract extraction. Visual acuity - left eye 20/80.

Left - Broad shallow subretinal fluid with areas of atrophic RPE. Hyperreflective consolidated material at the level of RPE (red arrow). (For interpretation of the references to colour in this figure legend, the reader is referred to the Web version of this article.)

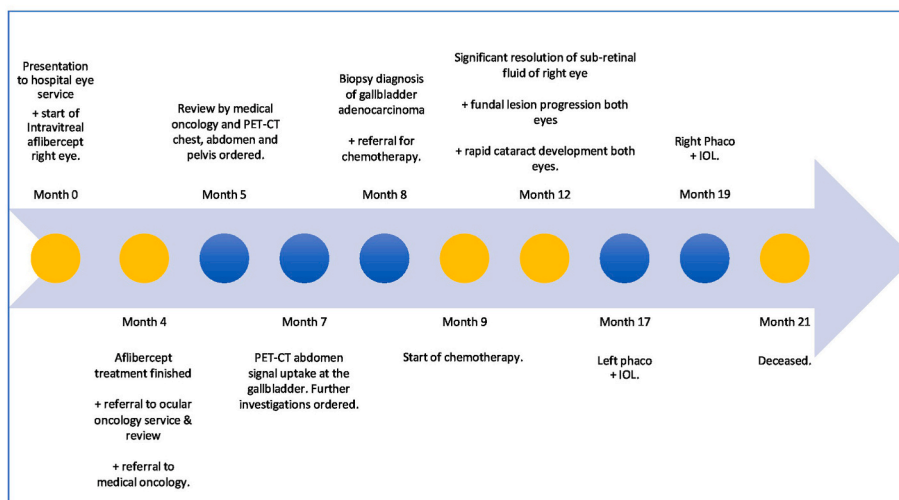


Fig. 5. Timeline of disease course from the beginning of visual symptoms to death. Phaco + IOL = Phacoemulsification and insertion of intra-ocular lens.

with intra-vascular and extra-vascular distribution will both not be removed efficiently and will have a faster rebound concentration in circulation after treatment^{14,15} At diagnosis, our patient was not treated with plasmapheresis as it was hoped that tumor treatment would control the BDUMP. Once plasmapheresis was reconsidered, it was contraindicated as it would have caused washout of her chemotherapy.

Our patient's FNA immunohistochemistry demonstrated CK7 +ve and CK20-ve adenocarcinoma. CK patterns indicate the primary site of adenocarcinomas when investigating a tumor of unknown origin. CK7+/CK20- satisfies tumors of the biliary system and alongside the radiological result, supported the diagnosis of a primary gallbladder adenocarcinoma.

In the most recent comprehensive literature review published in 2017, the median age at presentation of BDUMP was 65 years, with a predilection for females.⁴ Female urogenital cancers and male lung cancers are the most frequent respectively. In 5 cases (9 %) the primary was never found. 44 % of patients presented with visual symptoms after being diagnosed with a primary tumor, but in almost half of patients, BDUMP diagnosis preceded or presented at the time of tumor diagnosis. Though prognosis is poor with mean survival following presentation of BDUMP of 15.7 months (range 10–60 months), its presence may be protective in that its investigation may expedite diagnosis of malignancy⁴

5. Conclusion

We present a case of BDUMP associated with gallbladder malignancy, a rarely published cause. We demonstrate the evolution of BDUMP over time with multimodal imaging both before and after commencement of chemotherapy, highlighting salient features that may aid early diagnosis and improve prognosis.

Patient consent

The deceased patient's next of kin has consented in writing to the publication of this case.

Funding

No funding or grant support

Authorship

All authors attest that they meet the current ICMJE criteria for Authorship.

CRedit authorship contribution statement

Shaman Dolly: Writing – review & editing, Writing – original draft, Visualization, Project administration. **Christiana Dinah:** Writing – review & editing, Visualization, Supervision, Investigation, Conceptualization.

Declaration of competing interest

The authors declare that they have no known competing financial interests or personal relationships that could have appeared to influence the work reported in this paper.

Acknowledgements

To the daughter of our patient who kindly gave permission to publish this for the education of all who may come across the disease.

References

- Gass JDM, Gieser RG, Wilkinson CP, Beahm DE, Pautler SE. Bilateral diffuse uveal melanocytic proliferation in patients with occult carcinoma. *Arch Ophthalmol*. 1990; 108(4):527–533. <https://doi.org/10.1001/archoph.1990.01070060075053>.
- Wolff-Rouendaal D de. Bilateral diffuse benign melanocytic tumors of the uveal tract. *Int Ophthalmol*. 1985;7(3-4):149–160. <https://doi.org/10.1007/bf00128361>.
- Weppelmann TA, Khalil S, Zafrullah N, Amir S, Margo CE. Ocular paraneoplastic syndromes: a critical review of diffuse uveal melanocytic proliferation and autoimmune retinopathy. *Cancer Control*. 2022;29, 10732748221144458. <https://doi.org/10.1177/10732748221144458>.
- Klemp K, Kiilgaard JF, Heegaard S, Norgaard T, Andersen MK, Prause JU. Bilateral diffuse uveal melanocytic proliferation: case report and literature review. *Acta Ophthalmol*. 2017;95(5):439–445. <https://doi.org/10.1111/aos.13481>.
- Breazzano MP, Bacci T, Wang H, Francis JH, Yannuzzi LA. Bacillary layer detachment in bilateral diffuse uveal melanocytic proliferation masquerading as neovascular AMD. *Ophthalmic Surg, Lasers Imaging Retin*. 2020;51(7):413–417. <https://doi.org/10.3928/23258160-20200702-07>.
- Rafei-Shamsabadi D, Schneider J, Trefzer L, Technau-Hafsi K, Meiss F, Ness T. Case report: blurred vision and eruptive nevi - bilateral diffuse uveal melanocytic proliferation with mucocutaneous involvement in a lung cancer patient. *Front Oncol*. 2021;11, 658407. <https://doi.org/10.3389/fonc.2021.658407>.
- O' Day R, Michalova K, Campbell WG. Bilateral diffuse uveal melanocytic proliferation associated with bladder cancer: a novel imaging finding. *Ophthalmic Surg, Lasers Imaging Retin*. 2019;50(8):525–528. <https://doi.org/10.3928/23258160-20190806-10>.

8. Ramtohul P, Engelbert M, Malclès A, et al. Bacillary layer detachment: multimodal imaging and histologic evidence of a novel optical coherence tomography terminology: literature Review and Proposed Theory. *Retina*. 2021;41(11):2193–2207. <https://doi.org/10.1097/iae.0000000000003217>.
9. Miles SL, Niles RM, Pittock S, et al. A factor found in the IgG fraction of serum of patients with paraneoplastic bilateral diffuse uveal melanocytic proliferation causes proliferation of cultured human melanocytes. *Retina*. 2012;32(9):1959–1966. <https://doi.org/10.1097/iae.0b013e3182618bab>.
10. Niffenegger JH, Soltero A, Niffenegger JS, Yang S, Adamus G. Prevalence of hepatocyte growth factor and autoantibodies to α -HGF as a new etiology for bilateral diffuse uveal melanocytic proliferation masquerading as neovascular age-related macular degeneration. *J Clin Exp Ophthalmol*. 2018;9(4):1–4. <https://doi.org/10.4172/2155-9570.1000740>.
11. Jansen JCG, Calster JV, Pulido JS, et al. Early diagnosis and successful treatment of paraneoplastic melanocytic proliferation. *Br J Ophthalmol*. 2015;99(7):943. <https://doi.org/10.1136/bjophthalmol-2014-305893>.
12. Mets RB, Golchet P, Adamus G, et al. Bilateral diffuse uveal melanocytic proliferation with a positive ophthalmoscopic and visual response to plasmapheresis. *Arch Ophthalmol*. 2011;129(9):1235–1238. <https://doi.org/10.1001/archophthalmol.2011.277>.
13. Jaben EA, Pulido JS, Pittock S, Markovic S, Winters JL. The potential role of plasma exchange as a treatment for bilateral diffuse uveal melanocytic proliferation: a report of two cases. *J Clin Apher*. 2011;26(6):356–361. <https://doi.org/10.1002/jca.20310>.
14. Lavine JA, Ramos MS, Wolk AM, et al. Heterogeneity of cultured melanocyte elongation and proliferation factor in bilateral diffuse uveal melanocytic proliferation. *Exp Eye Res*. 2019;184:30–37. <https://doi.org/10.1016/j.exer.2019.04.006>.
15. Alrashidi S, Aziz AA, Krema H. Bilateral diffuse uveal melanocytic proliferation: a management dilemma. *BMJ Case Rep*. 2014;2014(may22 1), bcr2014204387. <https://doi.org/10.1136/bcr-2014-204387>.